

# Mössbauer Investigation into the Reactions of Laser-evaporated Iron with Solid Oxygen at Low Temperatures

Y. Yamada\* and S. Hirayama

Department of Chemistry, Tokyo University of Science  
1-3 Kagurazaka, Shinjuku-ku, Tokyo 162-8601, Japan

Received: May 8, 2006; In Final Form: July 14, 2006

Laser-evaporated iron was deposited onto solid oxygen at 20 K to produce stratified samples consisting of Fe and O<sub>2</sub> layers. The Mössbauer spectra of these samples were acquired in order to investigate their oxidation states and chemical properties. The reaction produced the trivalent iron oxide particles whose size varied depending on the amount of Fe atoms deposited on the solid oxygen. Samples which had smaller amounts of Fe produced smaller iron oxide particles having superparamagnetism. When the sample was annealed at 293 K, the size of the iron oxide particles became larger due to aggregation. The sample with the thickest Fe-layer (180 nm) had a pure  $\alpha$ -Fe layer above the iron oxide layer, and the divalent iron oxide was formed after annealing at 293 K.

## 1. Introduction

Laser-ablation has been studied extensively and has been applied to many fields including the surface treatment of solids and the formation of thin films. Laser-evaporation is a very useful method for vaporizing various kinds of materials without causing radiant heating of surrounding materials. This makes it a convenient method for vaporizing materials near a cold head in a cryostat in order to study low-temperature reactions. We have previously reported reactions of laser-evaporated iron atoms with various reactant gases using a low temperature matrix isolation technique and Mössbauer spectroscopy.<sup>1-4</sup> The reactions of laser-evaporated iron atoms with oxygen produced FeO, Fe(O<sub>2</sub>), FeO<sub>3</sub>, (O<sub>2</sub>)FeO<sub>2</sub>, and OFeO which are reaction products of the gas phase and are trapped in a low temperature Ar matrix.<sup>5</sup> We have also reported laser-deposition of Fe metal onto Al or Si substrates at various temperatures,<sup>6</sup> and the formation of Fe-Al alloy or Fe-Si compounds was observed at the boundary between the Fe-films and the Al or Si substrate. Laser-deposition of hematite or magnetite onto Al substrates produced iron oxide films whose composition varied depending on the substrate temperature.<sup>7</sup> Thereby laser-deposition has the possibility of producing functional films whose chemical compositions and physical properties can be controlled.

Here, we report the reactions of laser-evaporated Fe with solid oxygen at 20 K. While the experimental setup is very similar to that employed in our previous matrix-isolation studies,<sup>5</sup> in this study the Fe atoms and O<sub>2</sub> gas are introduced alternately to the cold substrate in order to investigate the reaction of Fe with solid oxygen rather than the gas-phase reactions. This study is also a useful cross reference for the <sup>57</sup>Mn in-beam Mössbauer study of solid oxygen,<sup>8</sup> although the densities of <sup>57</sup>Fe and <sup>57</sup>Mn atoms are very different. Furthermore the reactions of laser-evaporated Fe atoms with solid oxygen may potentially provide a new technique for producing iron oxide particles or films.

## 2. Experimental

The experimental setup is almost the same as that employed

for our previous matrix-isolation studies.<sup>5</sup> Briefly, the second-harmonic laser light of a YAG laser pulse (Continuum Surelite, 532 nm, 200 mJ/pulse, 6 ns) was focused using a convex lens onto a <sup>57</sup>Fe metal target, and the iron atoms were laser-evaporated. One laser pulse evaporates  $2 \times 10^{-9}$  mol/pulse. The O<sub>2</sub> gas was introduced via an electric pulse valve onto the Al substrate (40  $\mu$ m) that was cooled down to 20 K using a closed-cycle helium refrigerator (Iwatani Cryomini-D). The deposition area was 3.4 cm<sup>2</sup>. The introduction of O<sub>2</sub> was accumulative, and the stratified sample consisting of O<sub>2</sub> layers and Fe layers was produced. The Mössbauer spectra of the sample were acquired using a <sup>57</sup>Co/Rh source in transmission geometry on a Wissel MDU1200 system.

## 3. Results and discussion

A schematic diagram of the stratified samples (**A**, **B**, **C**, **D**, and **E**) produced on the Al substrates at 20 K is shown in Figure 1. The thicknesses indicated in the figure are the equivalent values calculated from the amount of O<sub>2</sub> gas introduced and the amount of laser-evaporated <sup>57</sup>Fe atoms. For example, the sample **C** shown in Figure 1c consists of O<sub>2</sub> layers and Fe layers which have equivalent thicknesses of 1.7  $\mu$ m and 11 nm, respectively. There were 25 such double layers in order that for there to be sufficient <sup>57</sup>Fe amounts to acquire a good Mössbauer spectrum; the corresponding Mössbauer spectrum, which was acquired at 20 K, is shown in Figure 2c. The actual boundaries of the O<sub>2</sub> and <sup>57</sup>Fe layers are not smooth as indicated in the Figure 1. The actual boundaries would be rough and reactions might occur on the boundaries.

The thickest Fe layer was 180 nm (sample **A**, Figure 1a) and the Mössbauer spectrum for this sample (Figure 2a) has two sets of sextets, which correspond to iron oxide and  $\alpha$ -iron. The Mössbauer parameters of the iron/oxygen-stratified samples are summarized in Table 1. The iron oxide produced by these samples is trivalent Fe<sub>2</sub>O<sub>3</sub> with hyperfine magnetic fields of 422 kOe. The Mössbauer parameters of this iron oxide do not correspond to those of commonly known trivalent iron oxides crystals such as hematite ( $\alpha$ -Fe<sub>2</sub>O<sub>3</sub>) or maghemite ( $\gamma$ -Fe<sub>2</sub>O<sub>3</sub>). Structures of iron hydroxides and iron oxides are closely related because their surrounding natures of Fe atoms with O atoms are similar. Among commonly known iron hydroxides lepidocrocite ( $\gamma$ -FeOOH) is reported to have a small magnetic hyperfine field (458 kOe at 4.2 K),<sup>9</sup> but the iron oxide produced in

\*Corresponding author. E-mail: yyasu@rs.kagu.tus.ac.jp. Fax: +81-3-5228-8276

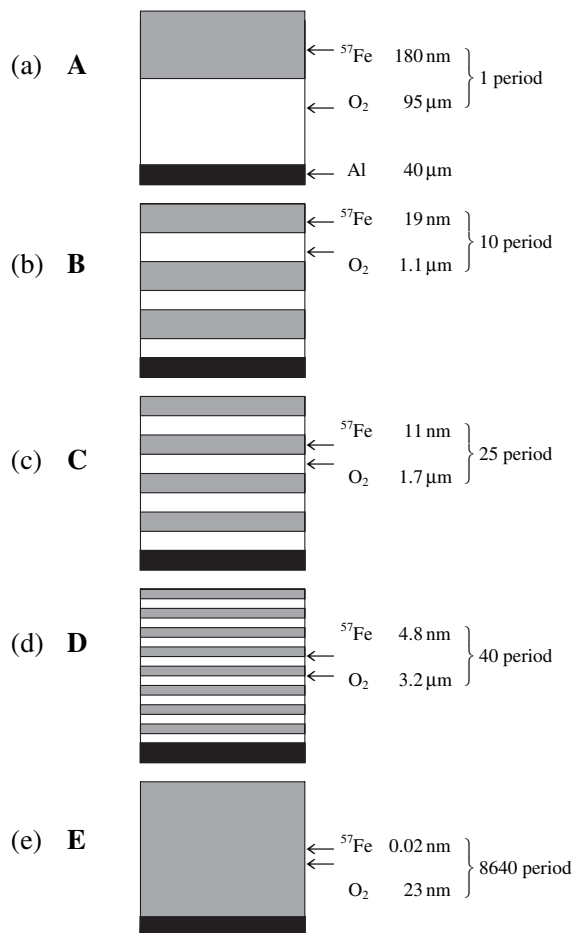


**Figure 1.** Schematic diagram of stratified samples (A, B, C, D, and E) consisting of  $^{57}\text{Fe}$  and  $\text{O}_2$  layers. The thicknesses indicated in the figure are the equivalent values calculated from the amount of  $^{57}\text{Fe}$  and  $\text{O}_2$  introduced.

this study has an even smaller magnetic hyperfine field. This small hyperfine magnetic field (422 kOe) may be attributed to large defects in its crystal structure or to small particle size.  $^{57}\text{Fe}$  reacted with  $\text{O}_2$  to form iron oxides at the interface of the  $^{57}\text{Fe}$  and  $\text{O}_2$  layers, and the  $^{57}\text{Fe}$  atoms that did not react with  $\text{O}_2$  were deposited to form an  $\alpha\text{-Fe}$  ( $H = 330$  kOe) layer on top of the iron oxide layer. From the area intensities of the Mössbauer spectrum, the thicknesses of iron oxide ( $\text{Fe}_2\text{O}_3$ ) and the pure iron ( $\alpha\text{-Fe}$ ) layers are calculated to be 70 and 110 nm, respectively.

The sample **B** with  $^{57}\text{Fe}$  layers having an equivalent thickness of 19 nm (Figure 1b and Figure 2b) does not show the sextet absorption of  $\alpha\text{-Fe}$ , instead doublet absorption was observed, which was assigned to superparamagnetic fine iron oxide particles. In addition, the sextet of iron oxide ( $\text{Fe}_2\text{O}_3$ ) was observed. The amount of  $^{57}\text{Fe}$  atoms introduced was not enough to form large  $\text{Fe}_2\text{O}_3$  particles, and hence the  $\text{Fe}_2\text{O}_3$  layer was too thin to stabilize the unreacted  $^{57}\text{Fe}$  layer. The sample **C** having thinner  $^{57}\text{Fe}$  layers (Figure 1c) has doublet absorption and a broad absorption exhibiting relaxation. The small size of the iron oxide particle gives a relaxation spectrum because of superparamagnetism. Although the particle size may have a size distribution, the relaxation spectrum is fitted by assuming it has a single relaxation time using Wickman's formula described in Reference 10; the relaxation time estimated by this method is 3.5 ns. The spectrum **D** shown in Figure 2d is also fitted by two components: a doublet and a relaxation component. The relaxation time of the superparamagnetic component is 2.6 ns, which is a narrower absorption than that estimated for the spectrum shown in Figure 2c. The spectrum shown in Figure 2e (sample **E**) is fitted by one doublet absorption with-

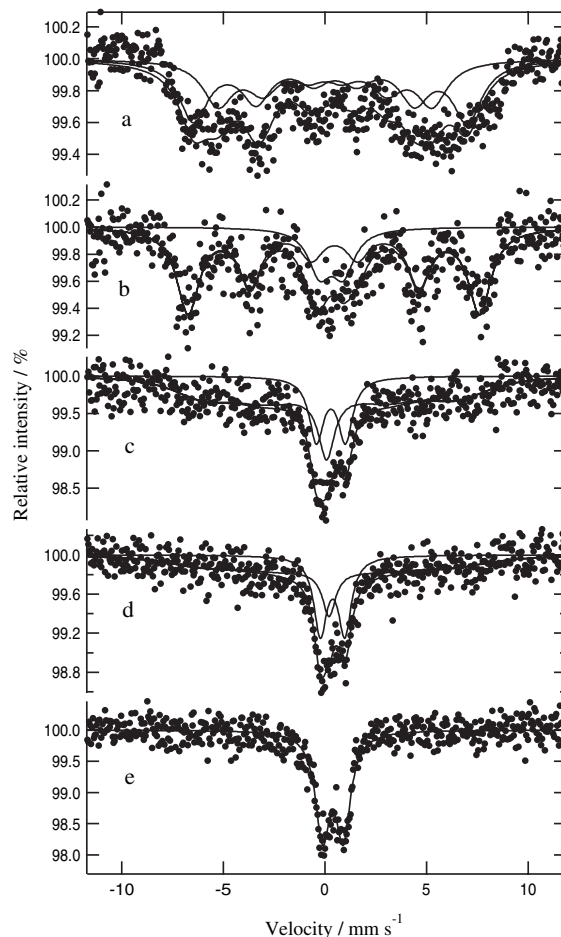


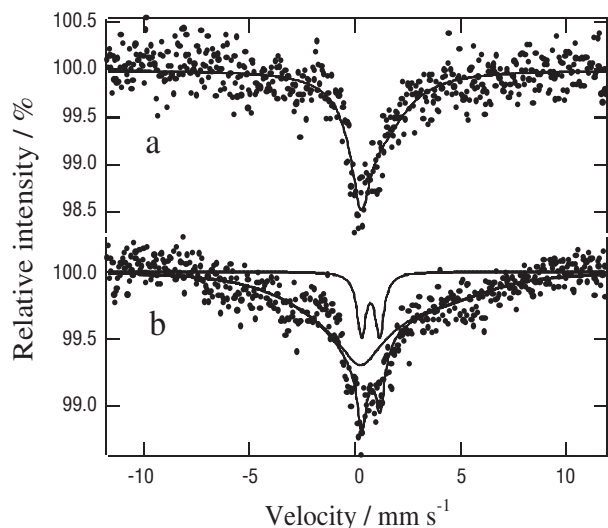
**Figure 2.** Mössbauer spectra of  $\text{Fe}/\text{O}_2$  stratified samples (A, B, C, D, and E) at 20 K. The equivalent thicknesses of  $^{57}\text{Fe}/\text{O}_2$  layers are (a) 180 nm/95  $\mu\text{m}$  (A), (b) 19 nm/1.1  $\mu\text{m}$  (B), (c) 11 nm/1.7  $\mu\text{m}$  (C), (d) 4.8 nm/3.2  $\mu\text{m}$  (D), and (e) 0.02 nm/23 nm (E).

out any magnetic hyperfine components. The doublet absorptions (for Figures 2b, c, d, and e) have almost identical Mössbauer parameters, and the area intensities become larger as the  $^{57}\text{Fe}$  layers become thinner. This doublet component may be attributed to fine particles of  $\text{Fe}_2\text{O}_3$  or to an amorphous structure even at 20 K. We have previously investigated the Mössbauer spectra of an iron oxide species isolated in a low-temperature Ar matrix,<sup>5</sup> and the  $\text{Fe}(\text{O}_2)$  had similar Mössbauer parameters ( $\delta = 0.35$  mm/s and  $\Delta E_Q = 0.96$  mm/s) to that of the doublet ( $\delta = 0.40$  mm/s and  $\Delta E_Q = 1.02$  mm/s) observed in this study. But the infrared spectrum of the sample acquired under the same conditions did not show any absorption bands corresponding to  $\text{Fe}(\text{O}_2)$  (979  $\text{cm}^{-1}$ ), and this species may not stabilize after the deposition of Fe atoms on the solid oxygen. Therefore we assigned the doublet to very small-sized oxide particles  $\text{Fe}_2\text{O}_3$ . The Mössbauer parameters for the doublet are in agreement with the parameters reported for superparamagnetic  $\gamma\text{-Fe}_2\text{O}_3$  particles reported in Reference 11 ( $\delta = 0.35$  mm/s and  $\Delta E_Q = 0.72$  mm/s). Mössbauer parameters of  $\epsilon\text{-Fe}_2\text{O}_3$  particles reported in literature<sup>12</sup> are not in agreement with our experimental results. The larger  $\Delta E_Q$  value of the observed doublet is due to the inhomogeneity of the size and crystallinity of the iron oxide  $\text{Fe}_2\text{O}_3$  particles.

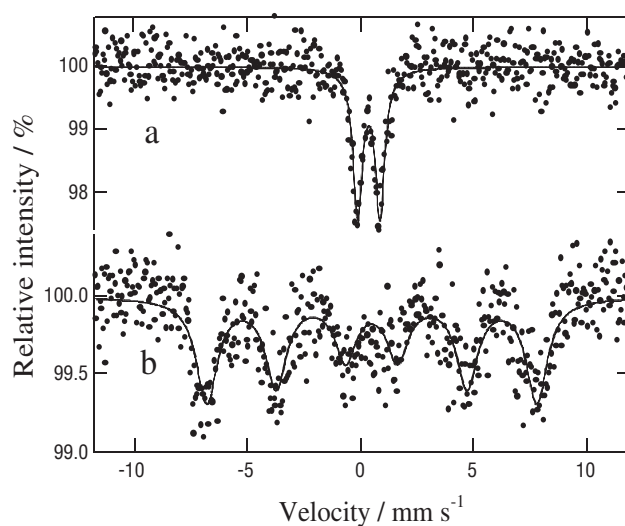
The sample **A** shown in Figure 2a, which had the  $\alpha\text{-Fe}$  layer, was annealed in order to investigate how its composition changed upon heating. The temperature of the sample was increased to room temperature (293 K), and  $\text{O}_2$  molecules were vaporized and evacuated, while iron species, which have a low vapor pressure, remained on the Al substrate. The Mössbauer spectrum acquired at room temperature (Figure 3a) shows a

**TABLE 1: Mössbauer parameters of iron/oxygen stratified samples at 20 K**

Sample	Temperature (K)	Component	$\delta$ (mm/s)	$\Delta E_Q$ (mm/s)	$H$ (kOe)	$\Gamma$ (mm/s)	relaxation time (ns)	Area intensity (%)
A	20	$\alpha$ -Fe sextet	0.00	0.00	330	1.83(20)	3.5(4)	57
			0.39(5)	-0.24(8)	422(3)	1.77(13)		43
B	20	doublet sextet	0.30(7)	1.11(11)	426(2)	0.32(2)	2.6(6)	21
			0.43(3)	-0.04(5)		1.29(5)		79
C	20	doublet relaxation	0.28(3)	1.45(6)	422	0.86(12)	3.5(4)	25
			0.17(9)	0.22(17)		0.16(6)		75
D	20	doublet relaxation	0.37(2)	1.20(4)	430(26)	0.76(9)	2.6(6)	37
			0.16(18)	-0.06(36)		0.15(7)		63
E	20	doublet	0.40(1)	1.02(2)		0.86(3)		100
A	293	relaxation	0.77(7)	1.10(15)	270(46)	0.42(5)	0.7(2)	100
A after annealing	20	doublet relaxation	0.70(2)	0.86(4)	270	0.50(5)	2.7(3)	14
			0.77	1.10		0.96(15)		86
B	293	doublet	0.33(1)	0.97(2)		0.49(3)		100
B after annealing	20	sextet	0.44(2)	0.01(5)	432(2)	1.07(6)		100

**Figure 3.** Mössbauer spectra of Fe/O<sub>2</sub> stratified sample **A** (<sup>57</sup>Fe/O<sub>2</sub> = 180 nm/95  $\mu$ m) observed at 293 K (a) and 20 K (b).

broad absorption, which is assigned to superparamagnetic iron oxide species having very small particle sizes. While the iron oxide particles may have a distribution of particle sizes and relaxation times, it is very difficult to fit the acquired relaxation spectrum by taking the size distribution of the iron oxide particles into account. Therefore the spectrum was fitted assuming a single relaxation time. The fitted result is shown in Figure 3a and the parameters obtained are given in Table 1; it has a large  $\delta$  value (0.77 mm/s) which is assigned to Fe(II) species. The magnetic hyperfine field was small ( $H = 270$  kOe) which is in good agreement with the small hyperfine field of Fe(II) species. The right shoulder of the absorption was attributed to the  $\Delta E_Q$  (1.10 mm/s) of the absorption with relaxation. The temperature of the sample **A** was then reduced to 20 K again. The Mössbauer spectrum at 20 K (Figure 3b) had a broader absorption with a longer relaxation time than that observed at room temperature (Figure 3a). The spectrum was fitted assuming that the broad component had the same  $\delta$ ,  $\Delta E_Q$ , and  $H$  values as those of Figure 3a, and it also had a doublet component. The relaxation time became longer (2.7 ns) and the doublet ( $\delta = 0.70$  mm/s and  $\Delta E_Q = 0.86$  mm/s) has the Mössbauer parameters assigned to a Fe(II) species. The spectrum acquired at 20 K did not have a component due to  $\alpha$ -Fe and it reacted with O<sub>2</sub> to form iron oxide when the temperature

**Figure 4.** Mössbauer spectra of Fe/O<sub>2</sub> stratified sample **B** (<sup>57</sup>Fe/O<sub>2</sub> = 19 nm/1.1  $\mu$ m) observed at 293 K (a) and 20 K (b).

was increased. Although iron oxide Fe<sub>2</sub>O<sub>3</sub> with magnetic hyperfine splitting was observed at 20 K before increasing the temperature (Figure 2a), the Mössbauer spectrum observed after annealing (Figure 3b) had a shorter relaxation time because of the smaller particle size, indicating that the Fe<sub>2</sub>O<sub>3</sub> particles did not aggregate to form larger particles on annealing. The divalent iron oxide FeO was produced by the reaction of pure Fe with O<sub>2</sub> and by the reduction of trivalent iron oxide Fe<sub>2</sub>O<sub>3</sub> with pure Fe.

Next, we annealed the sample **B** shown in Figure 2b to investigate the thermal reactions of a sample not having pure  $\alpha$ -Fe. When the temperature of the sample **B** was increased to room temperature 293 K, the solid O<sub>2</sub> layers evaporated and only the iron oxide remained on the Al substrate as large particles. The Mössbauer spectrum acquired at room temperature (Figure 4a) had only one doublet, which was assigned to the Fe<sub>2</sub>O<sub>3</sub> particles which exhibit superparamagnetism at high temperatures. The isomer shift ( $\delta = 0.33$  mm/s) of this doublet is that of trivalent iron oxide Fe<sub>2</sub>O<sub>3</sub> while it has a relatively large quadruple splitting ( $\Delta E_Q = 0.97$  mm/s) value. This sample **B** was again cooled to 20 K (Figure 4b), and the Mössbauer spectrum acquired at this temperature had a sextet absorption. The chemical composition or particle size may be the same as that for the sample in Figure 4a, and the only differences observed

were due to the different temperatures at which the Mössbauer spectra were acquired. Comparing the spectra of the samples **B** before (Figure 2b) and after annealing (Figure 4b), the doublet component disappeared and the component due to iron oxide  $\text{Fe}_2\text{O}_3$  with magnetic hyperfine splitting increased. On annealing the sample **B** (Figure 2b) and subliming the solid oxygen, the iron oxide particles aggregate to form larger  $\text{Fe}_2\text{O}_3$  particles which have magnetic hyperfine splitting at 20 K, although their size was not large enough to exhibit magnetism at room-temperature. Reduction of trivalent iron oxide  $\text{Fe}_2\text{O}_3$  to form divalent iron oxide FeO was not observed because there was no pure  $\alpha$ -Fe layer in this sample.

Laser-deposition of Fe onto solid oxygen at 20 K produced iron oxide  $\text{Fe}_2\text{O}_3$  particles, and the species obtained by matrix-isolation studies were not found even at low temperatures (20 K). The  $\text{Fe}_2\text{O}_3$  layer was formed up to thicknesses of 70 nm, and it had a small hyperfine magnetic field in the range 420 – 430 kOe. Laser-deposition of Fe onto solid  $\text{O}_2$  may provide a new method to produce small  $\text{Fe}_2\text{O}_3$  particles.

#### 4. Conclusion

Laser-evaporated Fe was deposited onto solid oxygen at 20 K. Samples having thinner Fe layers produced smaller particles of trivalent iron oxide  $\text{Fe}_2\text{O}_3$ . The measured Mössbauer parameters for  $\text{Fe}_2\text{O}_3$  particles do not correspond to those for known iron oxide crystals, and they may have a large number of defects. When the temperature of the sample was increased to 297 K, aggregation of the  $\text{Fe}_2\text{O}_3$  particles to form larger particles was observed. When there was a large amount of laser-deposited Fe present, a layer of pure  $\alpha$ -Fe formed on the  $\text{Fe}_2\text{O}_3$  layer. On annealing the sample at 293 K, reduction of the trivalent oxide  $\text{Fe}_2\text{O}_3$  to the divalent iron oxide FeO was observed

due to the reduction reaction with pure Fe. It was demonstrated that laser deposition of Fe onto solid oxygen produces particles of iron oxide having a novel structure, and that the particle size was determined by the amount of Fe deposited.

#### References

- (1) Y. Yamada, K. Katsumata, H. Shimasaki, Y. Ono, and K. Yamaguchi, *Bull. Chem. Soc. Jpn.* **75**, 227 (2002).
- (2) Y. Yamada, H. Shimasaki, Y. Okamura, Y. Ono, and K. Katsumata, *Appl. Radiat. Isot.* **54**, 21 (2001).
- (3) Y. Yamada and K. Katsumata, *Chem. Lett.* **2000**, 746 (2000).
- (4) Y. Yamada, *J. Nucl. Radiochem. Sci.* **1**, 75 (2000).
- (5) Y. Yamada, H. Shumino, Y. Okamura, H. Shimasaki, and T. Tominaga, *Appl. Radiat. Isot.* **52**, 157 (2000).
- (6) K. Namiki, D. Yokoyama, and Y. Yamada, *AIP Conf. Proc.* **765**, 114 (2004).
- (7) D. Yokoyama, K. Namiki, and Y. Yamada, *J. Radioanal. Nucl. Chem.* **268**, 283 (2006).
- (8) Y. Yamada, Y. Kobayashi, H. Ueno, M. K. Kubo, H. Watanabe, A. Yoshimmi, H. Miyoshi, D. Kameda, and K. Asahi, *RIKEN Accel. Prog. Rep.* **35** (2002).
- (9) E. Murad, *Phys. Chem. Minerals* **23**, 248 (1996).
- (10) H. H. Wickman and G. K. Wertheim, *Chemical Applications of Mössbauer Spectroscopy, Chapter 11*, Eds. V. I. Goldanski and R. H. Herber, Academic Press Inc. New York, (1968).
- (11) C. Musić, M. Gotić, S. Popović, and I. Czakó-Nagy, *Mater. Letters* **20**, 143 (1994).
- (12) E. Tronc, C. Chanéac, and J. P. Jolivet, *J. Solid State Chem.* **139**, 93 (1998).